ARL-MR-0999 • MAY 2019

# A Method for Performing Dynamic Tensile Extrusion of Materials at High Temperature

by Joseph Koby and Jeffrey Ball

## NOTICES

### Disclaimers

The findings in this report are not to be construed as an official Department of the Army position unless so designated by other authorized documents.

Citation of manufacturer's or trade names does not constitute an official endorsement or approval of the use thereof.

Destroy this report when it is no longer needed. Do not return it to the originator.

ARL-MR-0999 ● MAY 2019

# A Method for Performing Dynamic Tensile Extrusion of Materials at High Temperature

**by Joseph Koby**
*SURVICE Engineering*

**Jeffrey Ball**
*Weapons and Materials Research Directorate, CCDC Army Research Laboratory*

# REPORT DOCUMENTATION PAGE

*Form Approved*
*OMB No. 0704-0188*



| 1. REPORT DATE *(DD-MM-YYYY)* | 2. REPORT TYPE | 3. DATES COVERED (From - To) |
|---|---|---|
| May 2019 | Memorandum Report | 1 December 2018–31 January 2019 |

**4. TITLE AND SUBTITLE**
A Method for Performing Dynamic Tensile Extrusion of Materials at High Temperature

**5a. CONTRACT NUMBER**

**5b. GRANT NUMBER**

**5c. PROGRAM ELEMENT NUMBER**

**6. AUTHOR(S)**
Joseph Koby and Jeffrey Ball

**5d. PROJECT NUMBER**

**5e. TASK NUMBER**

**5f. WORK UNIT NUMBER**

**7. PERFORMING ORGANIZATION NAME(S) AND ADDRESS(ES)**
US Army Combat Capabilities Development Command
Army Research Laboratory*
ATTN: FCDD-RLW-LH
Aberdeen Proving Ground, MD 21005-5069

**8. PERFORMING ORGANIZATION REPORT NUMBER**
ARL-MR-0999

**9. SPONSORING/MONITORING AGENCY NAME(S) AND ADDRESS(ES)**

**10. SPONSOR/MONITOR'S ACRONYM(S)**

**11. SPONSOR/MONITOR'S REPORT NUMBER(S)**

**12. DISTRIBUTION/AVAILABILITY STATEMENT**
Approved for public release; distribution is unlimited.

**13. SUPPLEMENTARY NOTES**
ORCID ID(s): Joseph Koby, 0000-0003-4109-9660
* The work outlined in this report was performed while the US Army Research Laboratory (ARL) was part of the US Army Research, Development, and Engineering Command (RDECOM). As of 31 January 2019, the organization is now part of the US Army Combat Capabilities Development Command (formerly RDECOM) and is now called CCDC Army Research Laboratory.

**14. ABSTRACT**
Dynamic tensile extrusion is a well-established material characterization technique that involves firing a test projectile through a conical die. Our method adds the capability of performing extrusions after heating the projectile (and test barrel) with a 7-kW induction furnace. This new apparatus successfully extruded a 6.35-mm (0.25-inch) copper projectile to a diameter of 1.9 mm at a temperature of approximately 725 °C. The extruded copper fragments were recovered, mostly undamaged, using a ballistic gel block. We performed three tests at a projectile velocity of approximately 450 m/s, with one test done at room temperature as a control. Up to twice the amount of a given projectile will extrude through the die at high temperature when compared with the amount extruded from a room-temperature test.

**15. SUBJECT TERMS**
dynamic extrusion, high temperature, jetting, induction heating, copper

| 16. SECURITY CLASSIFICATION OF: | | | 17. LIMITATION OF ABSTRACT | 18. NUMBER OF PAGES | 19a. NAME OF RESPONSIBLE PERSON |
|---|---|---|---|---|---|
| a. REPORT | b. ABSTRACT | c. THIS PAGE | | | Joseph Koby |
| Unclassified | Unclassified | Unclassified | UU | 31 | 19b. TELEPHONE NUMBER (Include area code) (410) 278-0607 |

## Contents

## List of Figures

## List of Tables

## Acknowledgments

We would like to thank the following individuals for their contributions to this effort:

- Richard Summers and Jeffrey Welch for their technical assistance throughout the test program.
- Bob Borys and Colby Adams for their support during range operations.
- David Gray, RJ Spink, and Joe Colburn for providing much of the necessary diagnostic equipment for our use.
- Nathan Reichenbach and Phil Jannotti for their feedback and suggestions while assembling this manuscript.

# 1. Introduction

Dynamic tensile extrusion (DTE) is a well-established technique for characterizing materials under extreme conditions, together with more familiar methods such as Taylor anvil impact and split Hopkinson pressure bar tests. DTE involves firing a projectile of test material from a gas gun or powder gun, with the projectile passing through a conical die. The die reduces the projectile diameter, applying high-rate shear and tensile loading in the process. This allows for high-rate ductile-brittle transition and/or jetting behavior to be observed under well-controlled and easily repeated conditions.[1–4]

Previously, DTE has been done at room temperature, with any heated tests stopping at 250 °C.[5] The experiment described in this report features DTE at temperatures above 700 °C. This new method was developed and tested at the Army Research Laboratory's (ARL's)* Experimental Facility 167, operated by the Applied Physics Branch. The method is capable of reaching very high extrusion temperatures, while still recording projectile extrusion behavior and recovering the extruded material. This is accomplished by heating the gun barrel with an induction furnace immediately before firing. Barrel heating behavior is described, and the results of our initial proof-of-concept experiments with high-temperature copper extrusion are also discussed.

# 2. Methods

## 2.1 Range Configuration

A .25-cal. smoothbore barrel is used here to launch the projectiles for extruding. However, other calibers will also work if the projectile and die dimensions are scaled appropriately. Our testing scheme used copper projectiles because both raw material and earlier extrusion data are readily available.[1,6,7] The projectile was a right circular cylinder with a hemispherical nose, and a length-to-diameter ratio of 1. To extrude the projectile, an extrusion die is mounted along the shot line, roughly 750 mm from the muzzle.† Alignment of the die with the barrel is accomplished using a laser boresight and a mirror fixed to the exit side of the die. The die is properly positioned when the incident beam and return beam overlap. This die is made of heat treated A2 steel (BHN of 555) and features a 20° conical orifice, with

* As of February 2019, the US Army Research Laboratory has been renamed the US Army Combat Capabilities Development Command Army Research Laboratory (CCDC ARL).

† Normally, the extrusion die is mounted much closer to the muzzle, with only a small gap (~50 mm) for measuring projectile velocity. The excess distance was required to provide space for additional diagnostics for measuring projectile temperature in flight. Ultimately these diagnostics did not work as well as intended.

an exit diameter of 1.9 mm (0.075 inch). For a projectile of 6.35-mm (0.25-inch) diameter, this exit diameter equates to a 70% reduction in cross-sectional area. Schematics of the projectile and die are shown in Fig. 1.

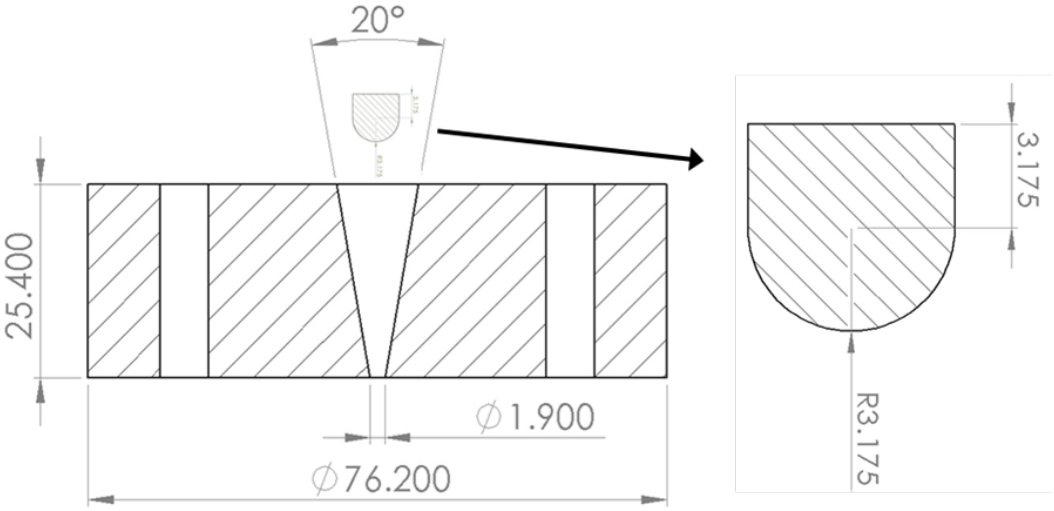


**Fig. 1 Extrusion die (left) and test projectile (right)**

Given the requirements for high-temperature operation, a powder gun was chosen over a gas gun for launching the projectiles. This eliminated the need for specialized pressure seals, heat sinking, and other advanced hardware that a gas gun would require when operating at 700 °C.

With a projectile mass of 23 gr (1.5 g) and a required velocity of 300–500 m/s, only 1–3 gr of propellant is needed per test. However, because this is such a small quantity of propellant, a chamber adaptor is needed to sufficiently reduce the ullage for reliable ignition and combustion. This adaptor is a solid piece of steel with the same dimensions as the chamber and a 3.175-mm (0.125-inch) hole drilled through the center for the propellant charge and primer. After load development tests, we determined a small rifle primer with 2 gr of Alliant Bullseye gave favorable results, with a typical muzzle velocity of around 450 m/s. This velocity was observed to be independent of barrel temperature.

## 2.2 Static Heating

To heat the projectile, a 7-kW induction heating coil is positioned around the barrel at the location of the projectile. This heating coil heats the barrel and the projectile inside, and the gun is fired once the needed temperature is reached. We do not heat the barrel all the way to equilibrium, since excessive heat would still reach the propellant. Instead, the barrel is heated for 30–60 s, depending on temperature requirements. Several heating cycles were performed on the test barrel at various

furnace settings in order to establish heating and cooling times. Temperatures were measured on the outer surface of the barrel, and inside the bore at the projectile, using type K thermocouples. Figure 2 shows the temperature profile for 60 s of heating, with the furnace set at full power.

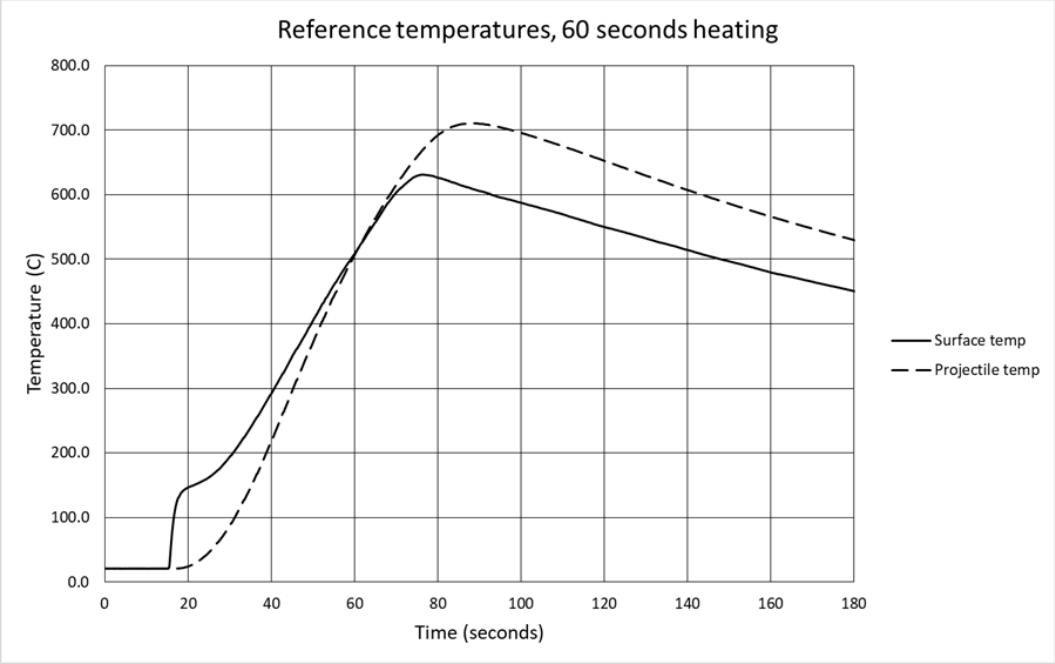


**Fig. 2 Temperature data for projectile and barrel exterior. The induction furnace was run for 60 s at full power (maximum coil current of 600 A).**

The "knee" in the surface temperature curve occurs because the induction furnace heats the thermocouple wire faster than the barrel, until the temperature reaches 150 °C. Once the barrel is hotter than 150 °C, the thermocouple begins to function normally. The in-bore probe did not exhibit this behavior, as the surrounding barrel shielded the probe.

Since heating tests like those in Fig. 2 do not involve firing the gun, it is possible to measure projectile temperature directly. During extrusion tests, projectile temperature cannot be measured, so the external barrel temperature is used to estimate the projectile temperature based on these earlier data. Therefore, during an extrusion test it is essential to run the furnace for the same amount of time, and at the same power settings, as during a static heating test.

## 2.3 Dynamic Testing

When loading the gun, it is necessary to position the projectile at least 45 mm (1.75 inches) downbore from the chamber. Otherwise the heating coil would be placed around the propellant charge, likely resulting in premature ignition. While

this downbore configuration results in less consistent projectile velocity, the variation is not grossly excessive (within ±5% of expected velocity). For a high-temperature shot, the gun is fired 10–15 s after the heating coil is deactivated. This delay is required to allow heat to finish diffusing inward to the projectile, maximizing the projectile temperature.

During firing, two high-speed cameras are positioned to record the projectile velocity. One camera records the projectile entering the die, and a second camera records the extruded material exiting the die. Fragment velocities, morphologies, and breakup behavior are observed and measured. Finally, a ballistic gel block is used for recovering the extruded fragments for further examination. This entire experimental setup is shown Fig. 3. Appendix A contains additional images of our test equipment.

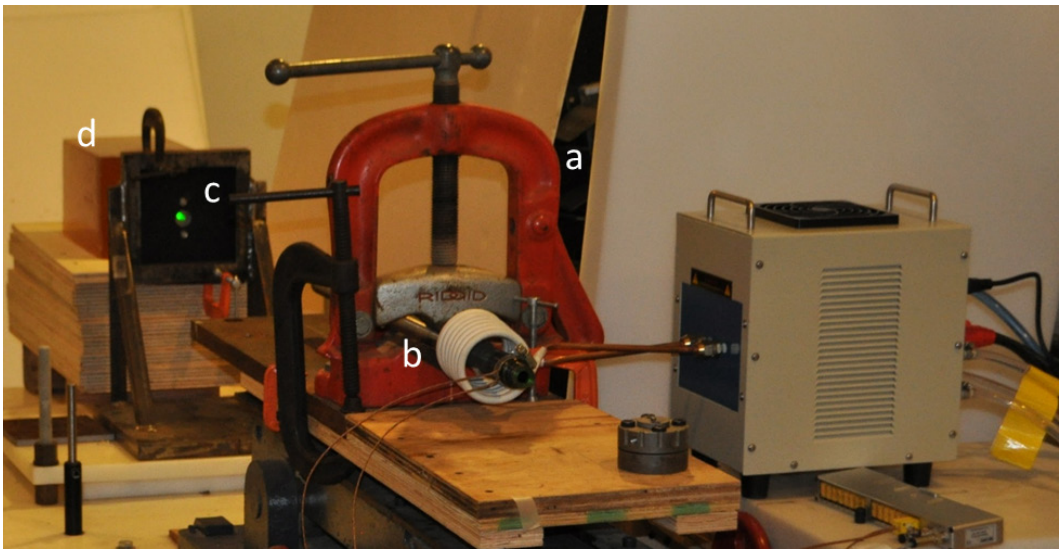


**Fig. 3 Range setup for high-temperature extrusion test. The large vice a) holds the test barrel, the induction coil is the white cylinder surrounding the test barrel b), the extrusion die is bolted to a vertical target stand c), and the gel block d) is located immediately behind the die.**

## 3. Extrusion Test Results

An example of a test projectile before and after extrusion is shown in Fig. 4. This particular extrusion was performed at room temperature, and is labeled as shot 676 in all tables and figures.

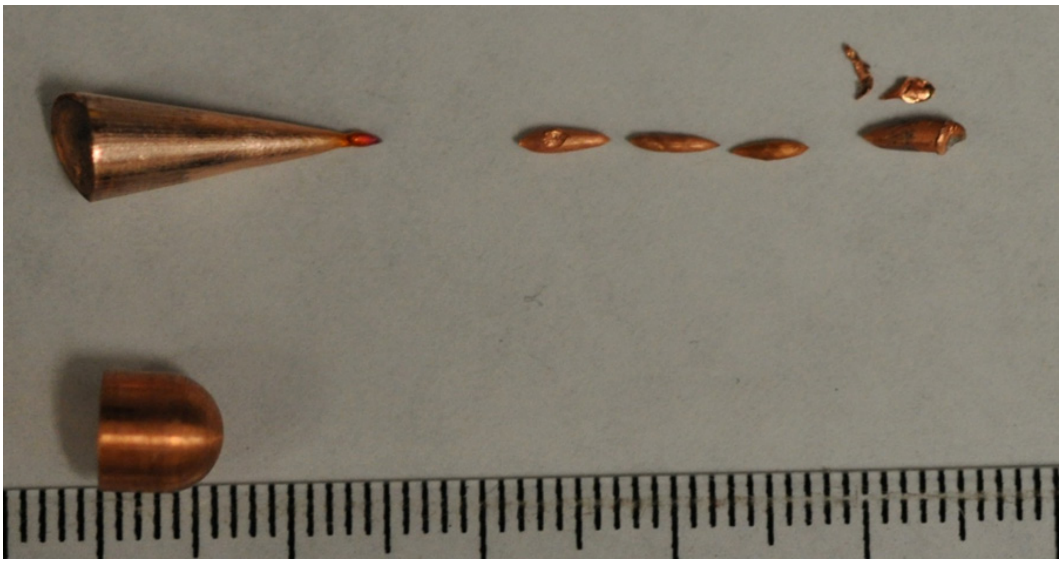

**Fig. 4 Test projectiles before and after extrusion and fragment recovery. Scale is in millimeters.**

Generally, most of the projectile remained in the die, while a small portion successfully exited the orifice as a jet. This jet then separated into a stream of individual particles, which travelled at ever-slower velocities. Extrusion velocities for all three experiments are found in Table 1. Shot 676 was a control test at room temperature, while shots 677 and 678 took place at approximately 700 °C. The entry and exit velocities for each test were measured from high-speed video data. Appendix B contains images from video data for all three shots.

**Table 1 Velocities of material entering and exiting extrusion die**

| Test number | Entry velocity (m/s) | Exit velocity (m/s) | | | | | | |
|---|---|---|---|---|---|---|---|---|
| | | Particle 1 | Particle 2 | Particle 3 | Particle 4 | Particle 5 | Particle 6 | Particle 7 |
| Shot 676 (20 °C) | 460 | 743 | 628 | 515 | 320 | 196 | . . . | . . . |
| Shot 677 (700 °C ) | 429 | 781 | 657 | 545 | 304 | 163 | . . . | . . . |
| Shot 678 (700 °C) | 446 | 812 | 751 | 670 | 542 | 364 | 303 | 152 |

Additionally, all recovered fragments were weighed. The masses of these recovered fragments are shown in Table 2. The initial projectile masses and total mass of extruded material are also included. Particles in Tables 1 and 2 are numbered in the order they exited the die (Particle 1 exits first, particle 2 second, etc.)

**Table 2 Mass of material entering and exiting the extrusion die**

| Test number | Entry mass (g) | Exit mass (g) | | | | | | | |
|---|---|---|---|---|---|---|---|---|---|
| | | Particle 1 | Particle 2 | Particle 3 | Particle 4 | Particle 5 | Particle 6 | Particle 7 | Mass thru die |
| Shot 676 (20 °C) | 1.488 | 0.072 | 0.033 | 0.006 | 0.019 | 0.017 | . . . | . . . | 0.147 |
| Shot 677 (700 °C) | 1.490 | 0.076 | 0.028 | 0.029 | 0.003 | 0.035 | . . . | . . . | 0.171 |
| Shot 678 (700 °C) | 1.480 | 0.058 | 0.043 | 0.023 | 0.043 | 0.006 | 0.039 | 0.055 | 0.267 |

External barrel temperatures for shots 677 and 678 are shown in Fig. 5, together with the heating results from Fig. 1. Given how similar the external temperatures are, it is safe to assume the projectile temperatures are equally consistent for each shot.

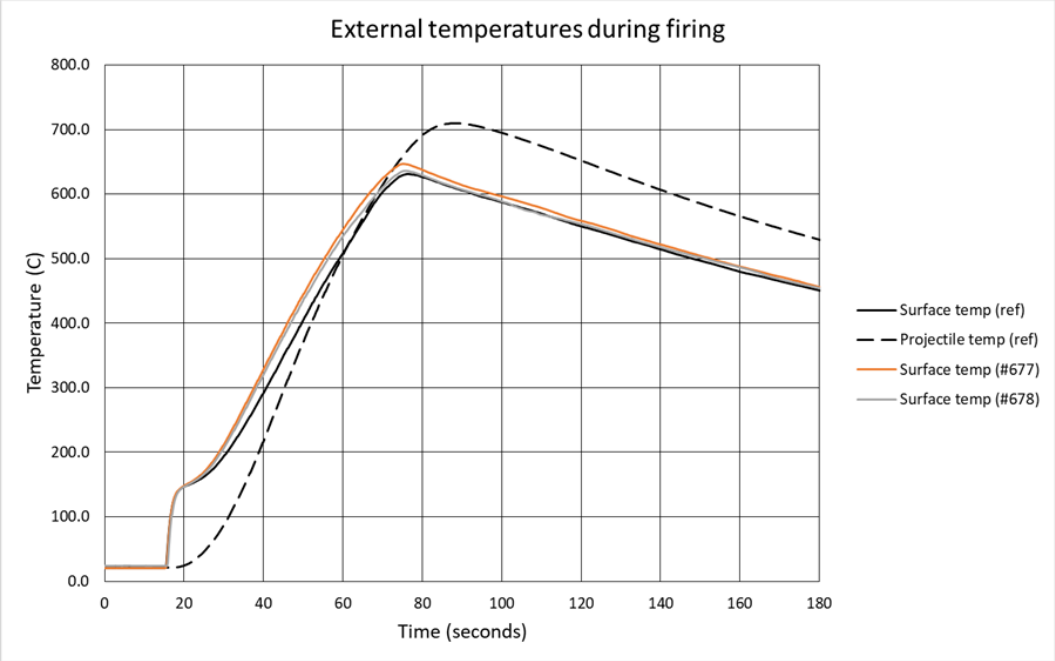


**Fig. 5 Barrel external temperatures recorded during extrusion experiments. Reference temperatures are from Fig. 1.**

## 4. Discussion

All three tests produced extruded jets of material. The room-temperature test (676) produced a jet that reached a length of 20 mm before breaking up. We observed different amounts of extrusion in each high-temperature test (677 and 678) with shot 677 extruding to 20 mm prior to breakup, as with the room-temperature

scenario, while shot 678 reached 40 mm before breakup. This breakup was consistently ductile, regardless of temperature, with all particles separating at thin points rather than larger fracture surfaces. Occasionally, a single particle began necking, but had too little energy available to completely separate.

Shots 676 and 677 also extruded similar masses of material, at 0.147 and 0.171 g, respectively. Meanwhile, shot 678 extruded 0.267 g, which is significantly more material. The cause of this difference between the two heated projectiles' behavior is inconclusive. Possible causes may be the presence or absence of projectile yaw at the die, or impact point variation between different shots. Mounting the barrel closer to the die in future tests should reduce this variability.

The entry and exit velocities from Table 1 are plotted together in Fig. 6. With an entry velocity of 400–450 m/s, the exit velocities tend to have a total spread of 500 m/s between the fastest and slowest particles. This spread increases to as much as 600 m/s during the high-temperature tests, particularly with shot 678. This spread clearly shows the leading particles are accelerated by the extrusion process, while the trailing particles are decelerated.

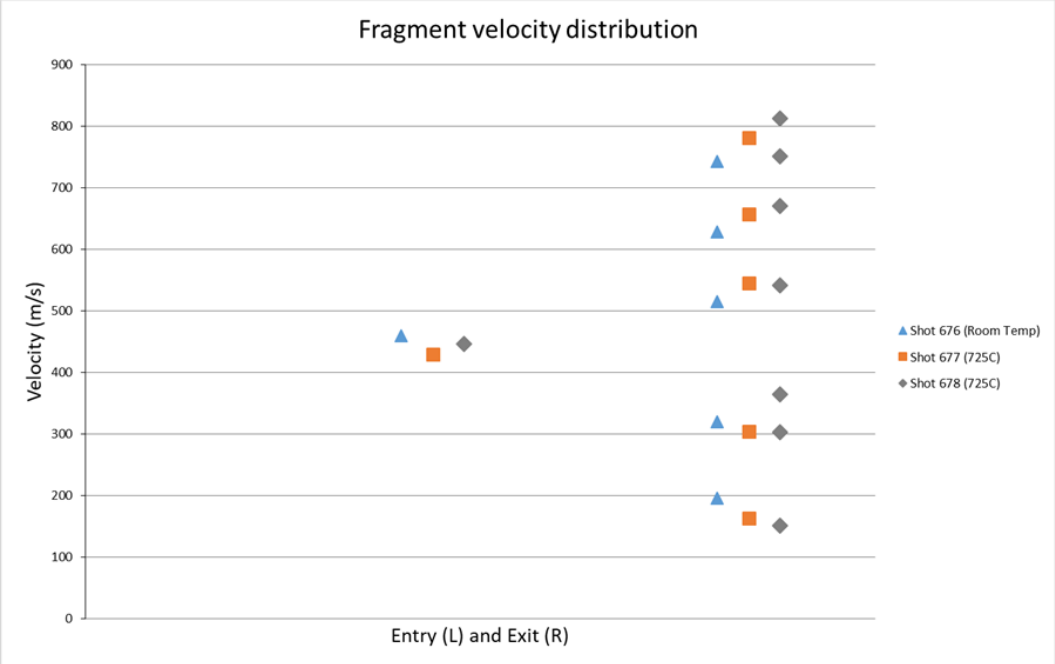


**Fig. 6 Velocity of entry and exit particles from the different dynamic tensile extrusion tests outlined in Table 1**

A noticeable gap in exit velocities is also seen, centered about the entry velocity of 450 m/s. This means that no particles exit the die at the same velocity as the projectile entered. Further study at different velocities is required to see if this velocity gap is a real effect or merely coincidental. This measurement would benefit

from more-refined methods of determining extrusion velocity, both during entry and exit, as high-speed video is more subjective than other diagnostics.

Figure 7 contains the particle mass distribution data from Table 2, together with the particles' exit velocities. Typically, the two most massive particles are the first and last to exit the die, although there is an exception with the room-temperature shot (676). In all three shots, however, the least massive particle is always adjacent to the gap at 450 m/s described earlier. As shown in Appendix C, these least massive particles are much smaller than the other particles recovered for a given shot.

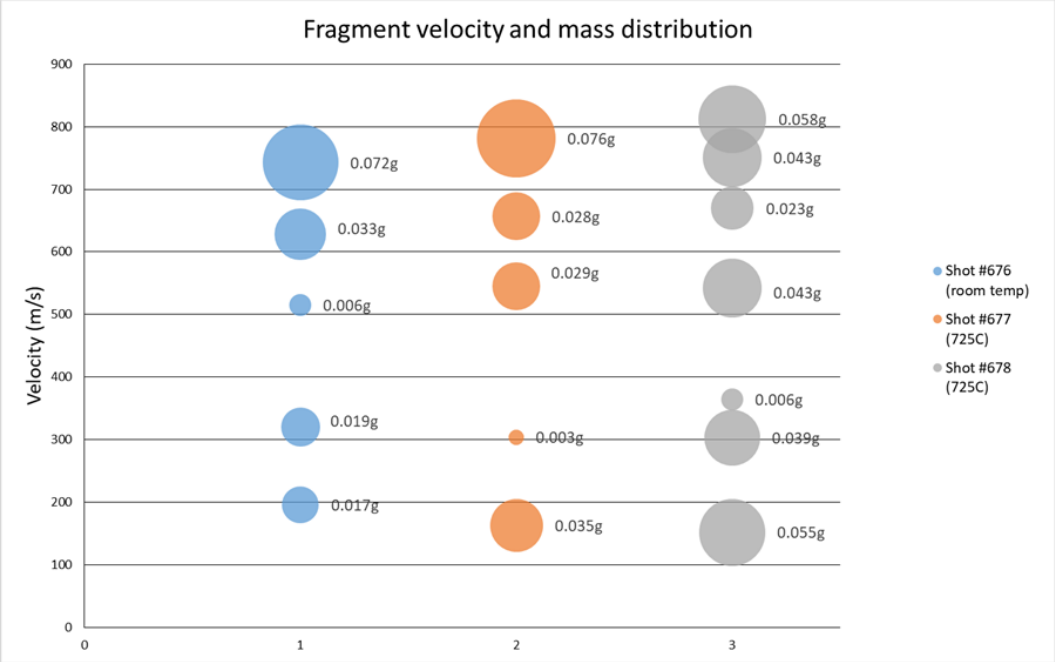


**Fig. 7 Mass of jet fragments from extrusion tests at room temperature and 700 °C**

A key source of error in fragment mass determination is the damage some particles experienced during recovery. This includes missing material, or conversely, the presence of small particles adhering to the main jet particles that we weighed. During extrusion, several very small (3 mg or less) particles are expelled ahead of the main jet. When these particles strike the ballistic gel block used for recovery, the gel cavitates, as soft tissue simulants are designed to do. Unfortunately, this cavitation sometimes allows a trailing particle to impact a leading particle without decelerating first. This impact either damages the particles or, in some cases, fuses the particles together. Several recovered jet particles were found with such impact damage; examples are shown in Fig. 8. Replacing the gel blocks with a suitable low density foam should reduce or eliminate this issue.

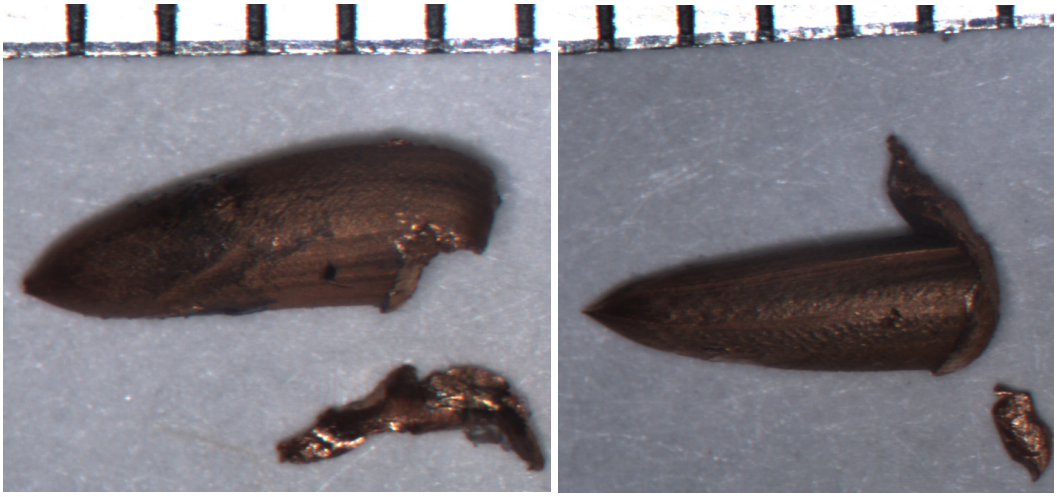

**Fig. 8 Examples of projectile damage during recovery, including missing material (left) and excess material (right). It was not clear if the small fragments originated from the specific large fragments shown here. Scale is in millimeters.**

## 5. Conclusions

A high-temperature version of the DTE test was successfully developed and tested at ARL. Using this method, copper projectiles were extruded at temperatures above 700 °C and underwent a cross-section reduction of 70%. The extruded material was successfully observed exiting the die, and these extruded fragments were also recovered, although in less than pristine condition. Extrusion results suggest that thermal softening will increase the amount of extruded material at high temperature; however, a larger test regimen would be needed before any definitive statements can be made.

Areas of further investigation would be to determine what effect a thinner barrel would have on heating (if any). We suspect that higher temperatures may be possible, since the same amount of power would be used to heat less material. Larger caliber projectiles, together with a matching larger extrusion die, would also be worth testing. It would be beneficial to determine if any scaling effects occur and the nature of these effects if they are seen. Larger projectiles would also be useful because the larger extruded samples would be easier to work with and more practical to examine further after extruding.

## 6. References


1. Gray GT III, Cerreta E, Yablinsky CA, Addessio LB, Henrie BL, Sencer BH, Burkett M, Maudlin PJ, Maloy SA, Trujillo CP, Lopez MO. Influence of shock prestraining and grain size on the dynamic-tensile-extrusion response of copper: experiments and simulation. In: Furnish MD, Elert M, Russell TP, White CT, editors. Proceedings of the Conference of the American Physical Society Topical Group on Shock Compression of Condensed Matter; 2005 July 31–Aug 5; Baltimore, MD. AIP Conference Proceedings. 2006;845:725–728.

2. Cao F, Cerreta EK, Trujillo CP, Gray GT III. Dynamic tensile extrusion response of tantalum. Acta Materialia. 2008;56(19):5804–4807.

3. Escobedo JP, Cerreta EK, Trujillo CP, Martinez DT, Lebensohn RA, Webster, Gray GT III. Influence of texture and test velocity on the dynamic, high-strain, tensile behavior of zirconium. Acta Materialia. 2012;60(11):4379–4392.

4. Furmanksi J, Trujillo C, Martinez DT, Gray GT, Brown E. Dynamic-tensile-extrusion for investigating large strain and high strain rate behavior of polymers. Polymer testing. 2012;31(8):1031–1037.

5. Escobedo JP, Cerreta EK, Martinez D, Trujillo C, Lebensohn R, Gray II GT. Influence of temperature on the dynamic tensile behavior of zirconium. Metallurgical and Materials Transactions A. 2014;45(13):5877–5882.

6. Bonora N, Testa G, Ruggiero A, Iannitti G, Mortazavi N, Hörnqvist M. Numerical simulation of dynamic tensile extrusion test of OFHC copper. Journal of Dynamic Behavior of Materials. 2015;1(2):136–152.

7. Burkett M, Clancy S. Eulerian hydrocode modeling of a dynamic tensile extrusion experiment. In: Schäfer F, Hiermaier S, editors. Proceedings of the 11th Hypervelocity Impact Symposium; 2010 Apr 11–15; Freiburg, Germany.

# Appendix A. Experimental Setup

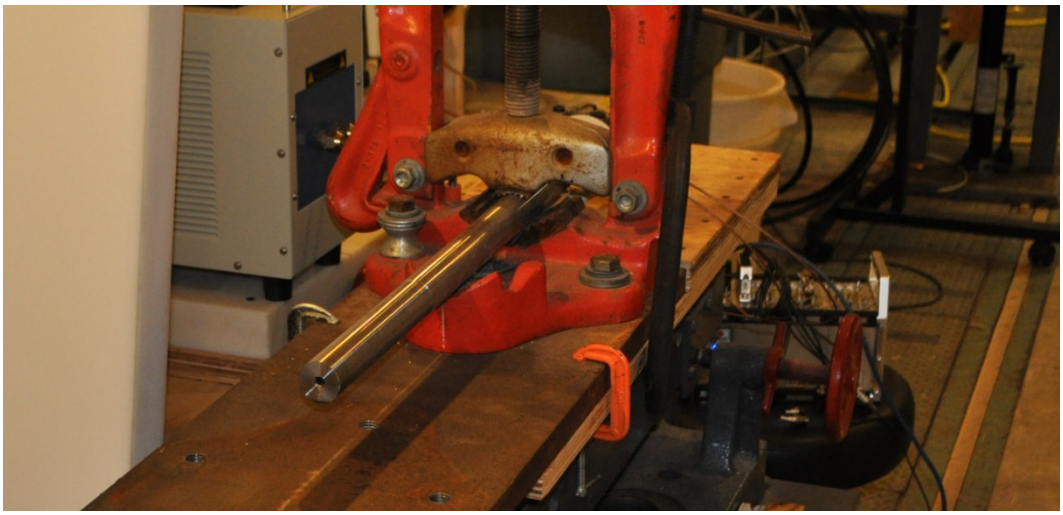

**Fig. A-1 Mounted test barrel**

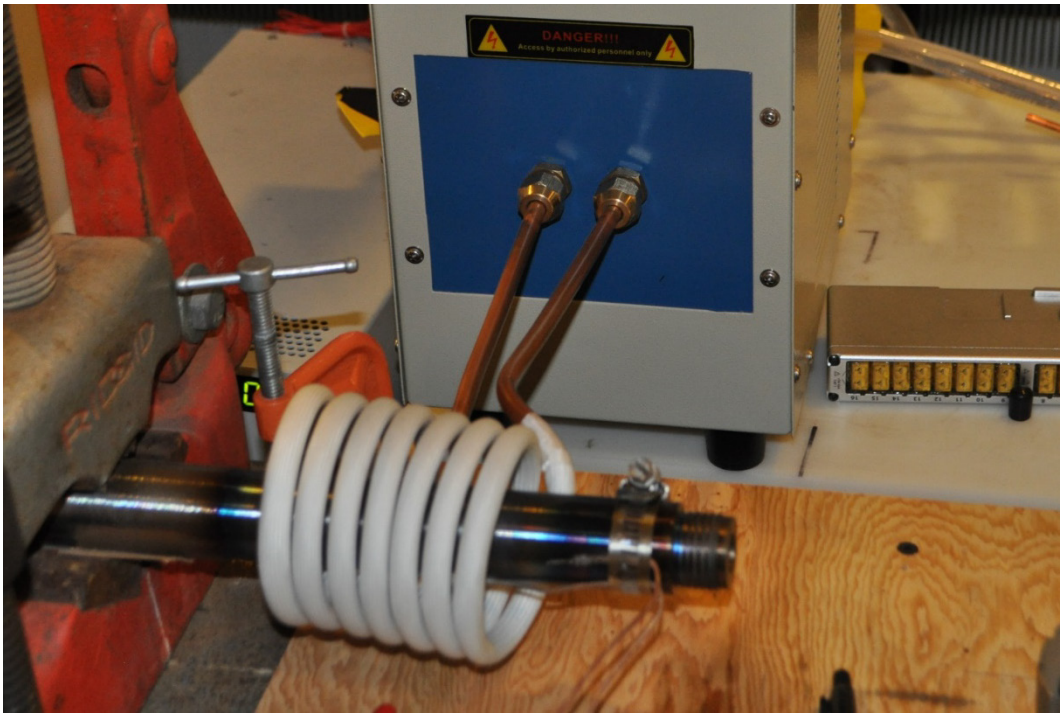


**Fig. A-2 Induction coil and barrel**

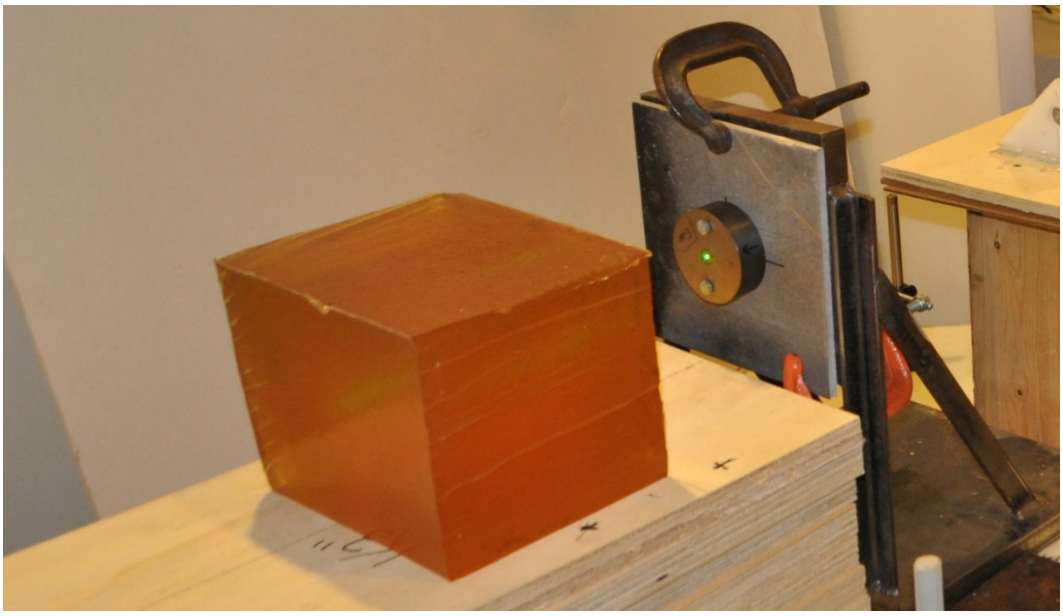

**Fig. A-3 Extrusion die and gel block**

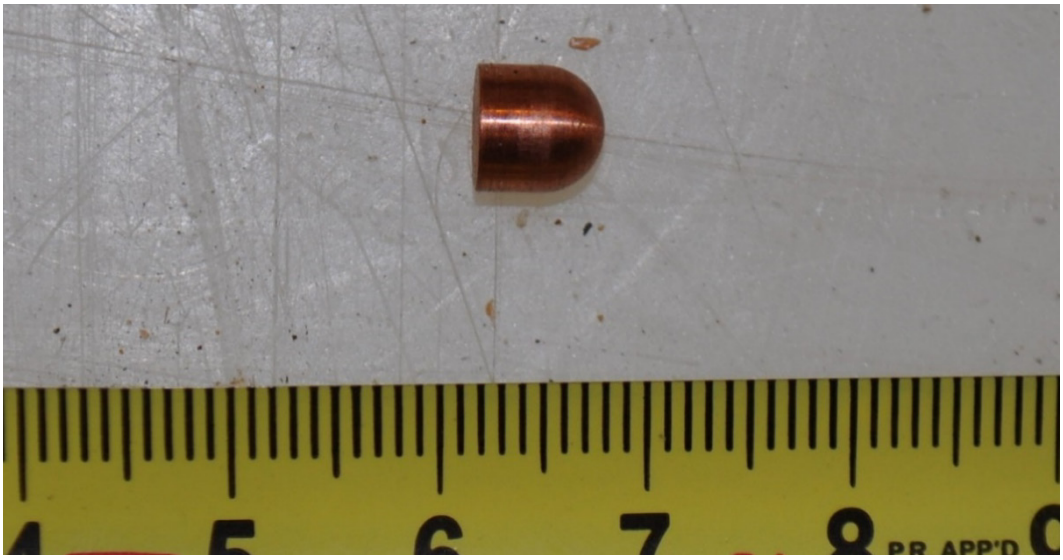

**Fig. A-4 Copper test projectile. Numbered scale is in centimeters (small marks are millimeters).**

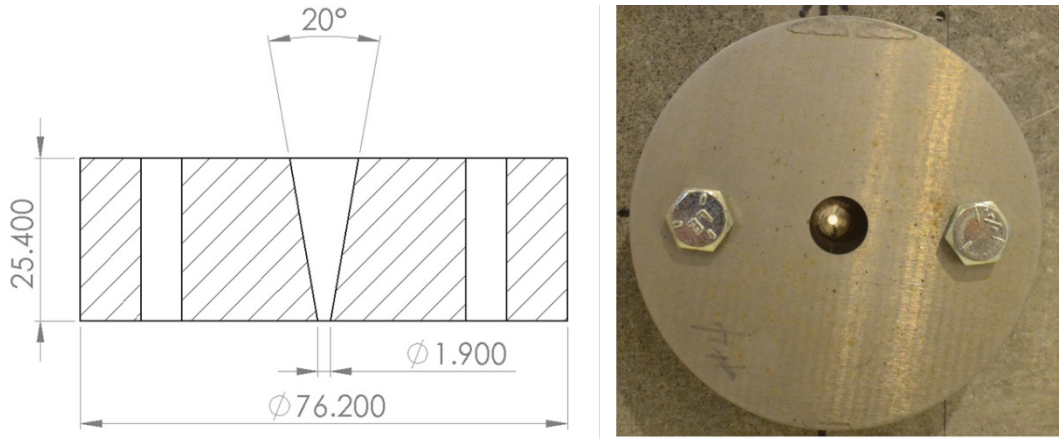


**Fig. A-5 Extrusion die with schematic**

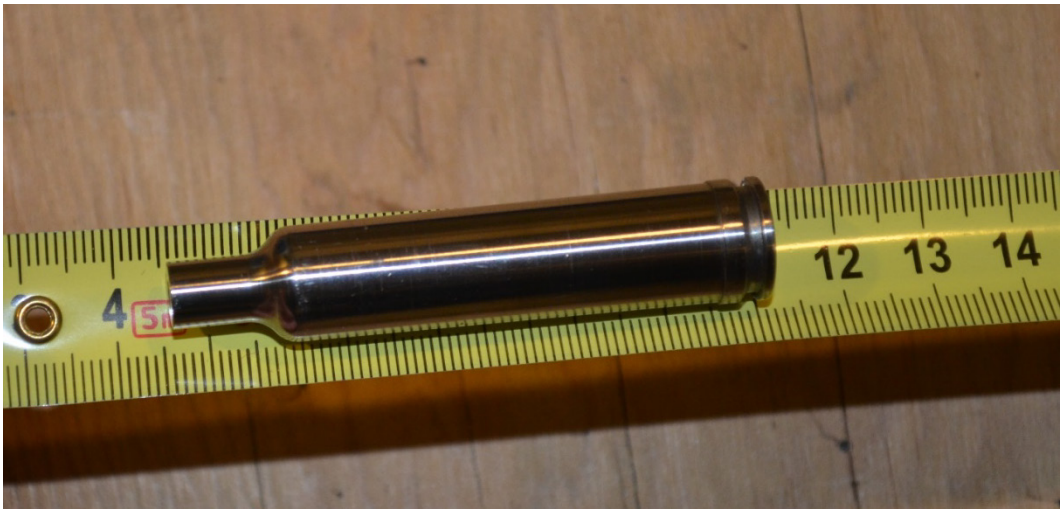


**Fig. A-6 Chamber adaptor, used for reducing ullage with light propellant charges. Numbered scale is in centimeters.**

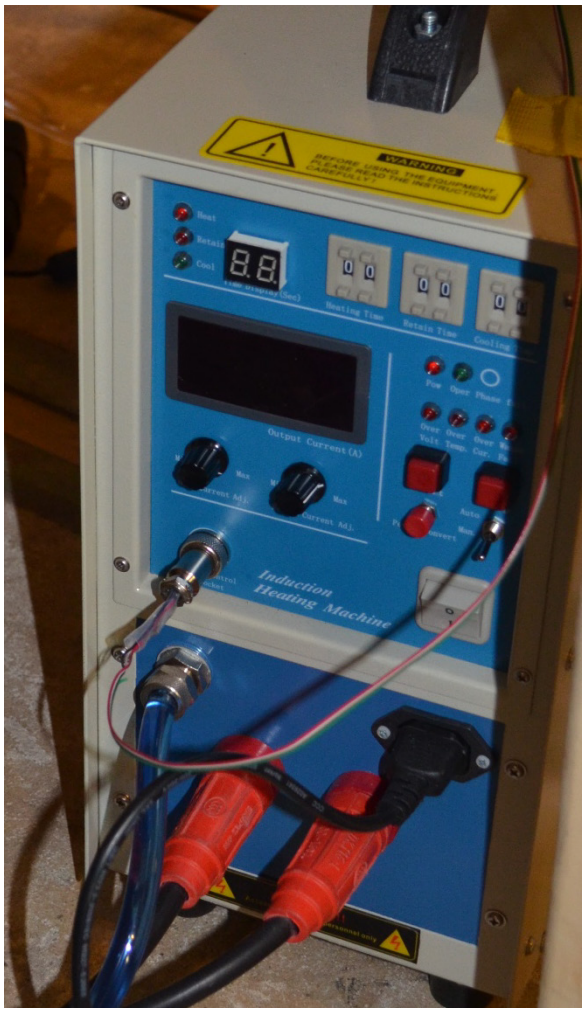


**Fig. A-7 Induction furnace control panel**

## Appendix B. High-Speed Video Images

High-speed video data for the three tests discussed in this report are shown in Figs. B-1 through B-6.

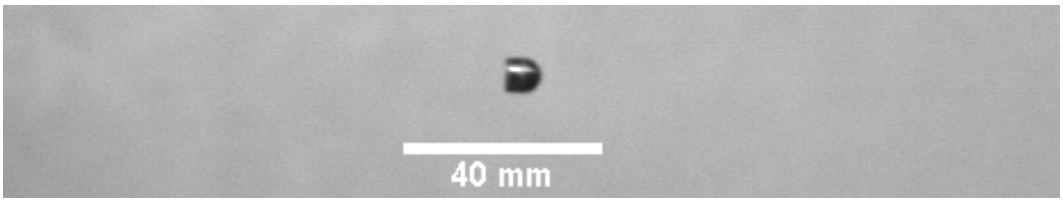


**Fig. B-1 Copper projectile before entering die (Shot 676, 20 °C)**

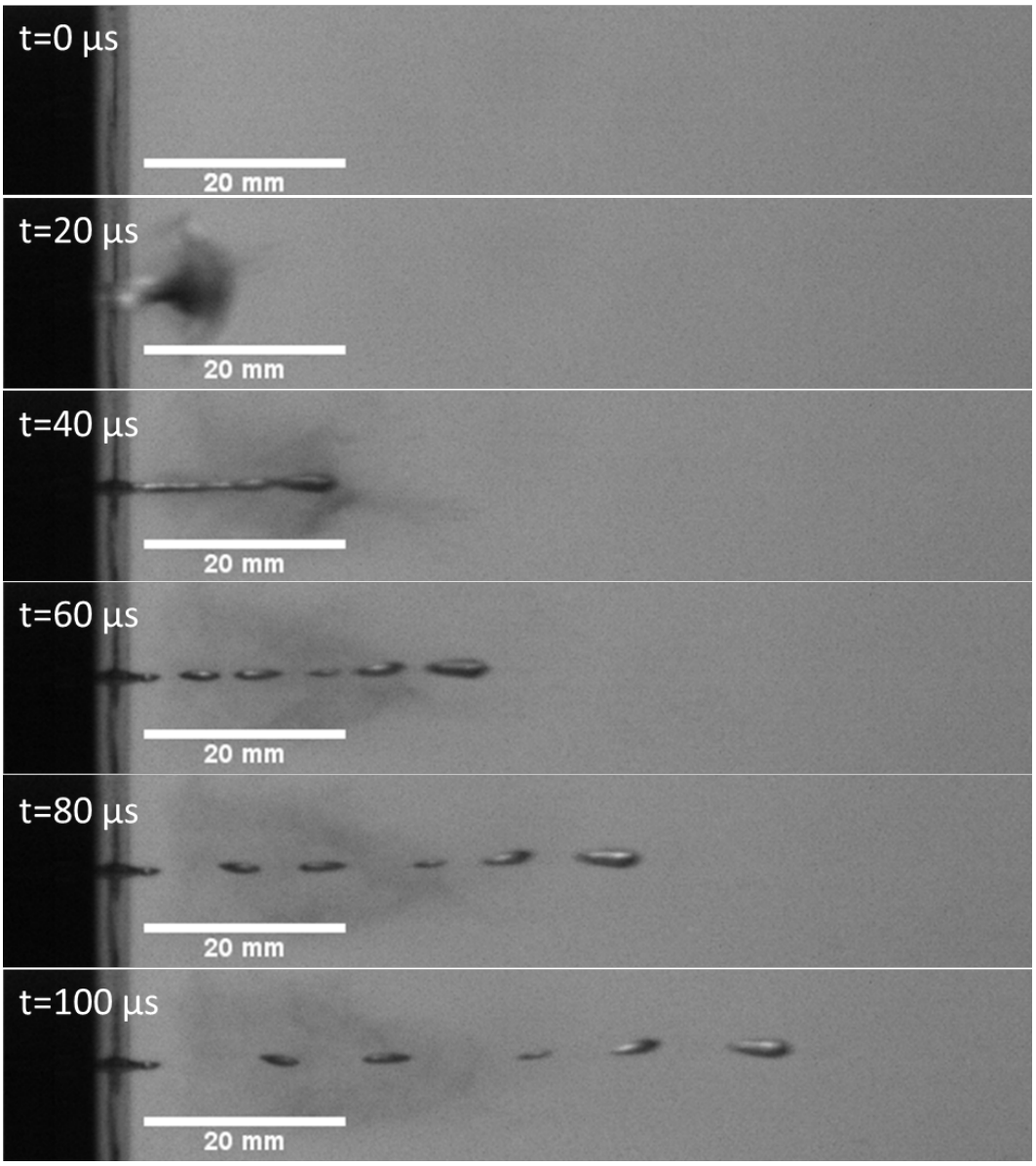


**Fig. B-2 Extruded copper exiting die (Shot 676, 20 °C)**

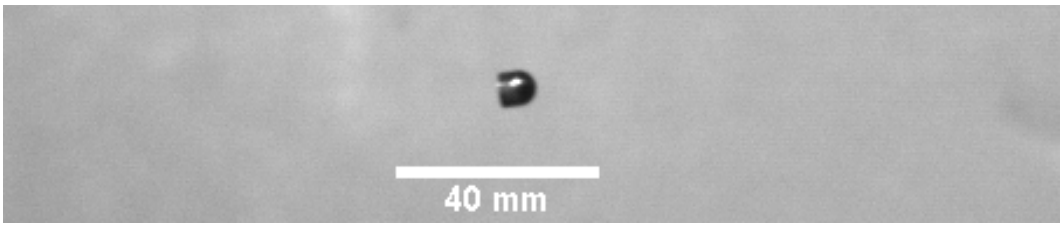


**Fig. B-3 Copper projectile before entering die (Shot 677, 700 °C)**

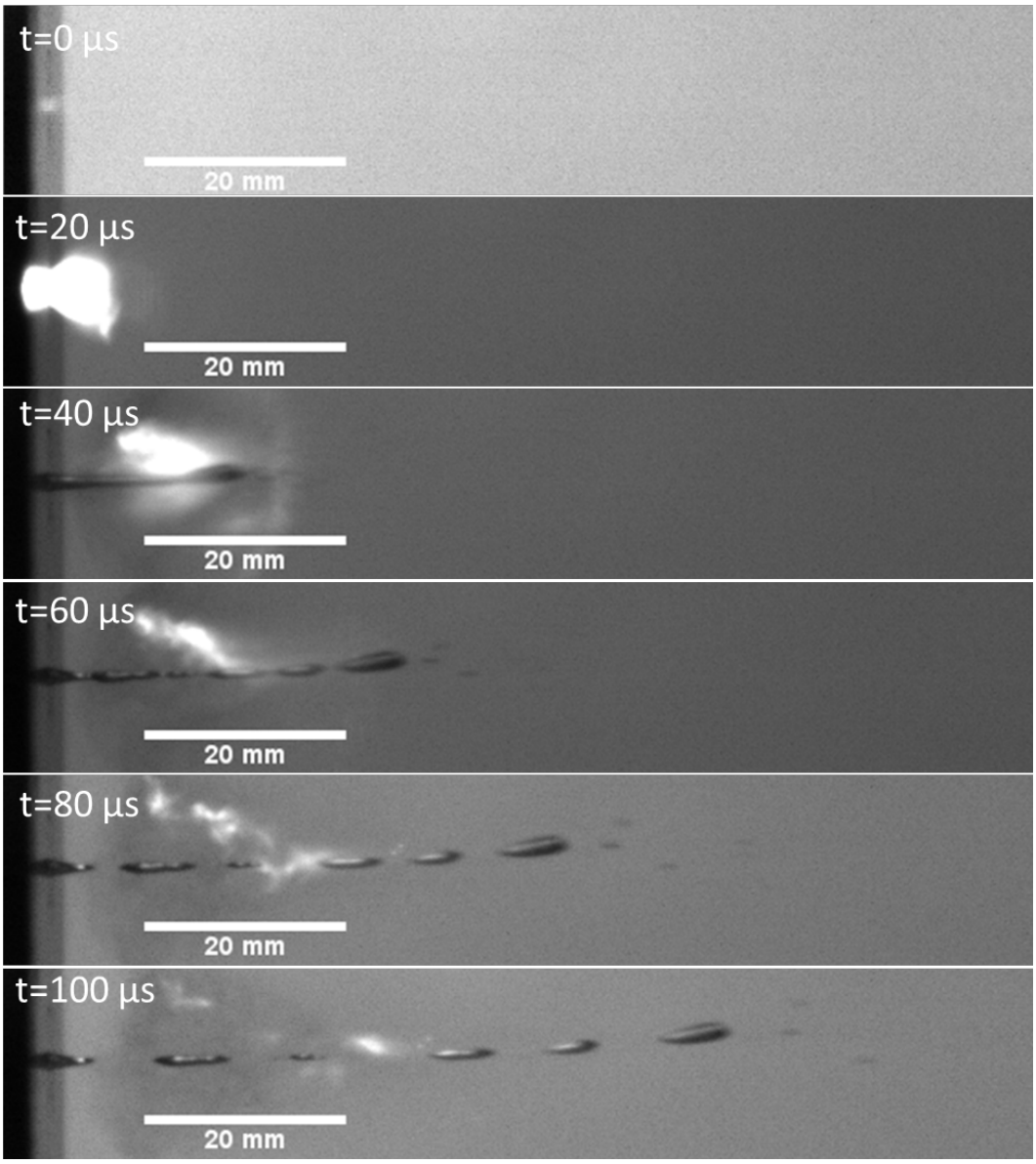


**Fig. B-4 Extruded copper exiting die (Shot 677, 700 °C)**

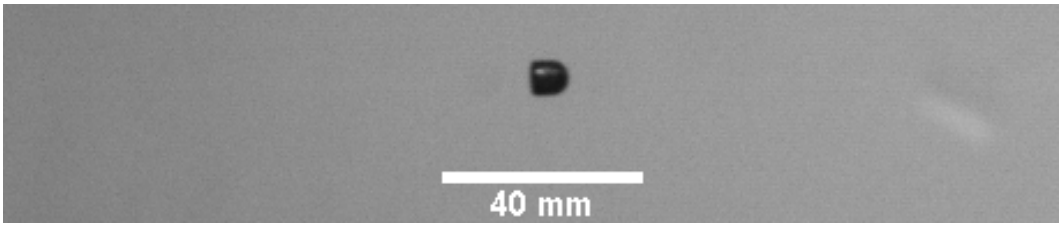


**Fig. B-5 Copper projectile before entering die (Shot 676, 700 °C)**

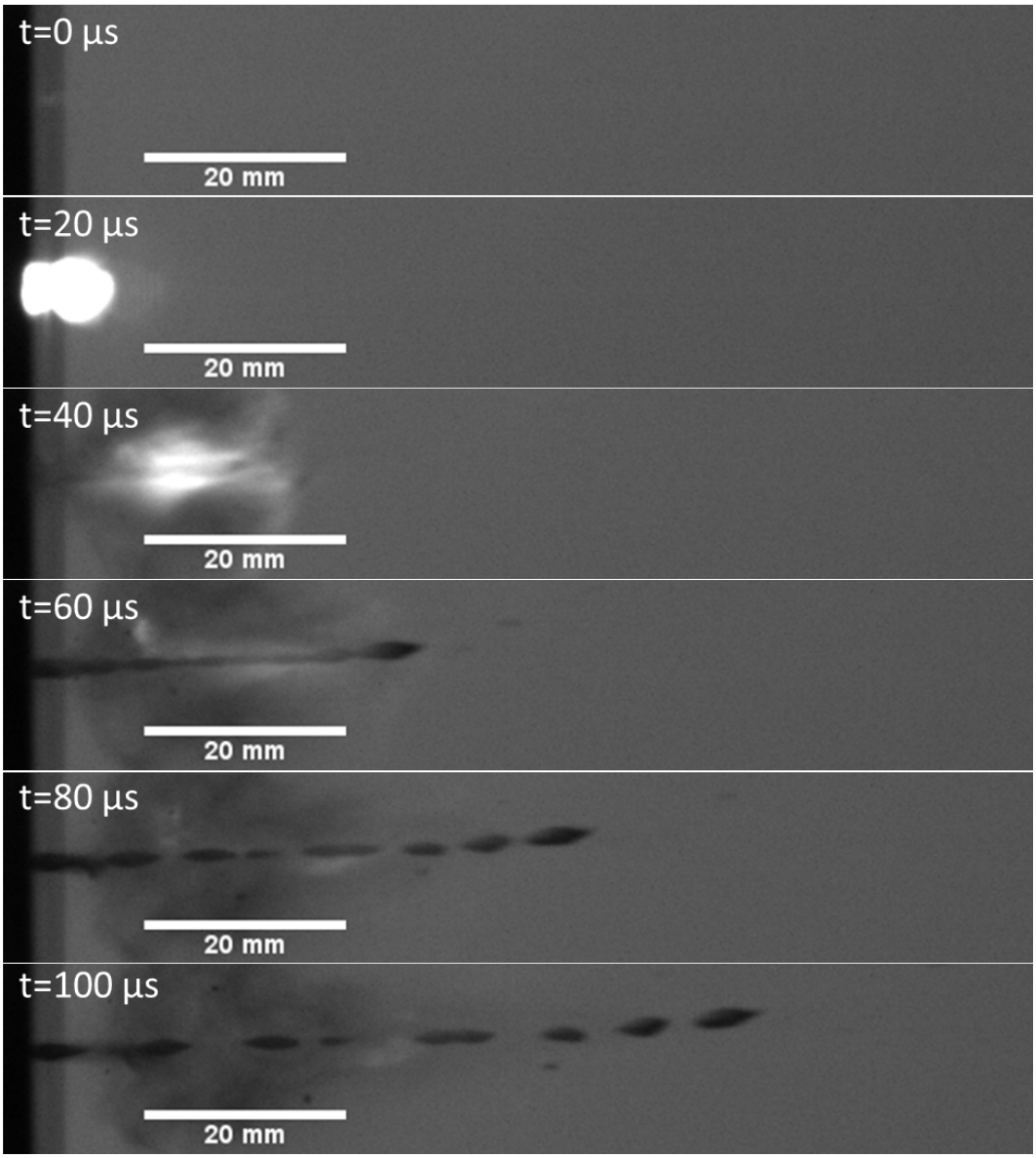


**Fig. B-6 Extruded copper exiting die (Shot 678, 700 °C)**

## Appendix C. Recovered Extruded Particles

Figures C-1 through C-4 are images of the material recovered after the extrusion tests described in the main text of this report. The scales in all images are in millimeters.

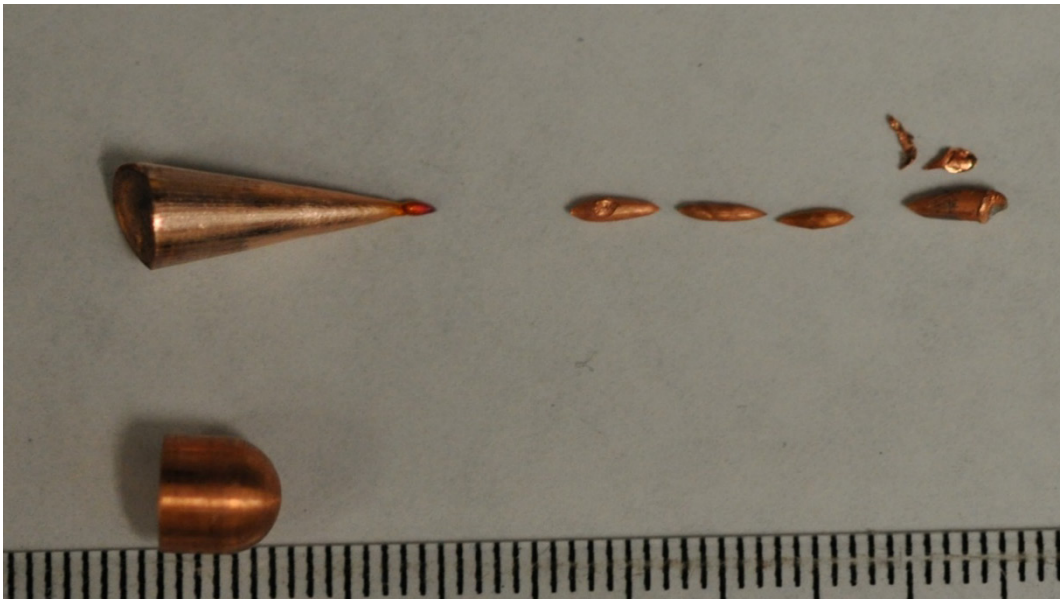

**Fig. C-1 Copper projectile before and after extruding. Fragments were taken from Shot 676 (room temperature.) Scale at bottom of image in millimeters.**

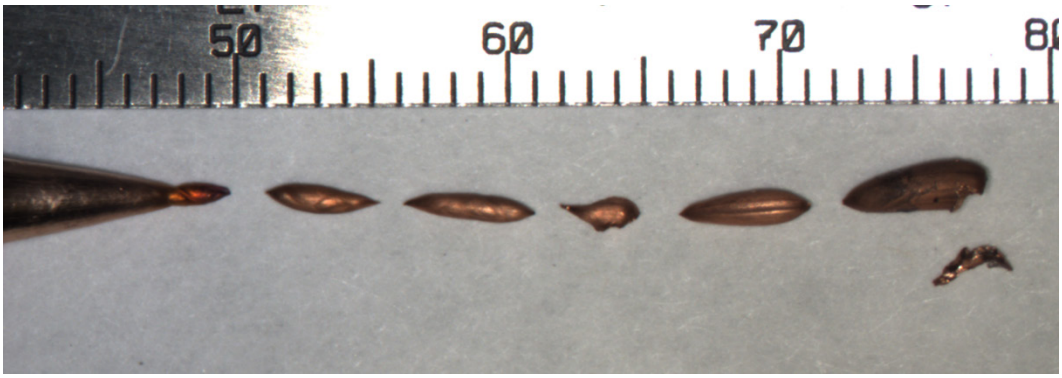


**Fig. C-2 Microscope image of fragments from Shot 676**


**Fig. C-3 Microscope image of fragments from Shot 677**

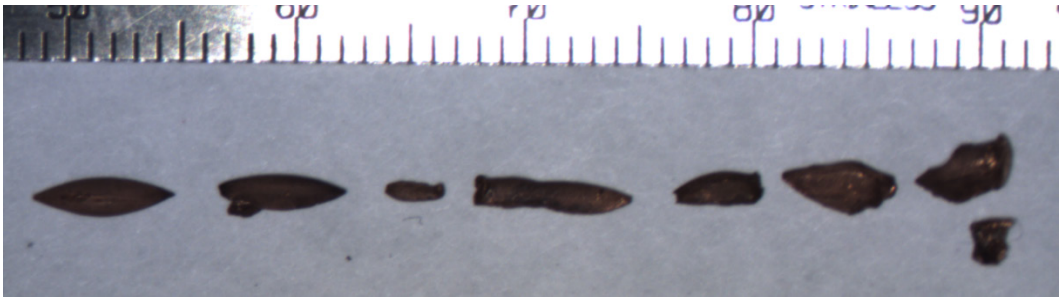

**Fig. C-4 Microscope image of fragments from Shot 678**

1 (PDF) DEFENSE TECHNICAL INFORMATION CTR DTIC OCA

2 (PDF) CCDC ARL
IMAL HRA
RECORDS MGMT
FCDD RLD CL
TECH LIB

1 (PDF) GOVT PRINTG OFC
A MALHOTRA

3 (PDF) ARDEC
FCDD ACM E
A PETROCK
FCDD ACM EF
P ROTTINGER
P REDNER

3 (PDF) LANL
GT GRAY
L HULL
M BURKETT

5 (PDF) CCDC ARL
FCDD RLW LH
J KOBY
R SUMMERS
FCDD RLW MF
A GIRI
K DARLING
FCDD RLW PA
J BALL